Pergamon

Geochimica et Cosmochimica Acta, Vol. 67, No. 5, pp. 955–965, 2003
Copyright © 2003 Elsevier Science Ltd
Printed in the USA. All rights reserved
0016-7037/03 $30.00 + .00

PII S0016-7037(02)00996-1

Surface alteration of arsenopyrite (FeAsS) by *Thiobacillus ferrooxidans*

R. A. JONES,[1] S. F. KOVAL,[2] and H. W. NESBITT[1,*]

[1]Department of Earth Sciences, University of Western Ontario, London, ON N6A 5B7, Canada
[2]Department of Microbiology and Immunology, University of Western Ontario, London, ON N6A 5C1, Canada

(*Received May* 30, 2001; *accepted in revised form March* 27, 2002)

Abstract—The surface of arsenopyrite was characterized after acidic, oxidative leaching in the presence of the bacterial species Thiobacillus ferrooxidans. Polished single-crystal grains of arsenopyrite were reacted for 1, 2, and 3 weeks with *T. ferrooxidans* suspended in a solution (pH 2.3) of essential salts ($MgSO_4 \cdot 7H_2O$, $[NH_4]_2SO_4$, KH_2PO_4, and KCl). Abiotic control experiments were conducted in identical solutions. Reaction between arsenopyrite and *T. ferrooxidans* in the essential salts solution produced a uniform solid $FePO_4$ overlayer (~0.2 μm thick) on the arsenopyrite surface within 1 week. The overlayer was detected visually by scanning electron microscopy (SEM) and chemically by X-ray photoelectron spectroscopy (XPS). It could not be distinguished by energy-dispersive X-ray analyses. No overlayer formed in the abiotic control. The uniform thickness and lateral continuity of the overlayer suggest an inorganic origin promoted by bacterial production of Fe^{3+}. Iron released from arsenopyrite was oxidized by bacteria and subsequently precipitated with PO_4^{3-} (from the essential salts), forming ferric phosphate. After 2 and 3 weeks, SEM images revealed a roughened arsenopyrite surface, and XPS depth profiles indicated a progressively thicker phosphate overlayer and continued oxidation, diffusion, and dissolution of arsenopyrite beneath the overlayer. After only 1 week, the cells were isolated from the arsenopyrite surface by the uniform overlayer. Therefore, bacteria need not be attached to arsenopyrite to promote rapid reaction, and the mechanism of alteration at the arsenopyrite surface must have been inorganic. Because the delicate overlayer did not prevent continued alteration of arsenopyrite, $FePO_4$ may not be an effective barrier to oxidation in the tailings environment. The $FePO_4$ coating has likely formed in other experiments using these bacteria but was not detected because analytical techniques were not sufficiently surface sensitive to identify a separate, compositionally distinct overlayer. Some previous experimental results thus may be misleading or inapplicable to the tailings environment. *Copyright © 2003 Elsevier Science Ltd*

1. INTRODUCTION

Arsenopyrite (FeAsS) is one of the minerals commonly discarded in mine wastes. Its oxidation products include oxyacids of As and S (such as H_3AsO_3, H_3AsO_4, and H_2SO_4) that are toxic to the environment in high concentration (Nesbitt et al., 1995). The rate of oxidation and dissolution of arsenopyrite and other sulfide minerals is increased by the metabolic processes of bacteria; thus, acid and toxic elements are rapidly released (Nordstrom and Southam, 1997). The bacterium *Thiobacillus ferrooxidans* was chosen for this study because of its well-documented ability to flourish in mine tailings or other acidic oxidizing environments and its ability to oxidize arsenopyrite. A few other bacteria are also known to oxidize arsenopyrite, including *Pseudomonas arsenitoxidans* (Ilyaletdinov and Abdrashitova, 1981) and *Sulfolobus* sp. (Groudeva et al., 1986; Ngubane and Baecker, 1990), but their effects on arsenopyrite and their roles in mine tailings have not been studied as extensively as those of *T. ferrooxidans*. *T. ferrooxidans* is a chemolithoautotroph; i.e., it extracts energy from chemical reactions rather than light, metabolizes minerals or inorganic solutes rather than organic matter, and fixes CO_2. It oxidizes either Fe or S, and derives energy by reducing O_2 and consuming H^+ to form H_2O. Biologic consumption of Fe^{2+} from arsenopyrite and production of Fe^{3+} may affect the oxidative dissolution of arsenopyrite by inorganic mechanisms.

Ehrlich (1964) reported that *Thiobacillus* increased the rate of oxidation of arsenopyrite, which resulted in precipitates of iron arsenite and arsenate, and later studies further examined the alteration of arsenopyrite by *Thiobacillus* (e.g., Collinet and Morin, 1990; Mandl et al., 1992; Tuovinen et al., 1994; Sampson and Blake, 1999). However, in each of these studies, powdered arsenopyrite reacted with bacteria in suspension, and solution chemistry or bulk secondary products were analyzed, not the arsenopyrite surface. By analysis of these final products, one can only infer the reactions that occurred, whereas analysis of the reacted mineral surface gives greater insight into chemical changes occurring at the interface.

Several analytical studies of the inorganic alteration process of arsenopyrite surfaces have been conducted (Buckley and Walker, 1988; Richardson and Vaughan, 1989; Nesbitt et al., 1995; Fernandez et al., 1996; Maddox 1996; Nesbitt and Muir, 1998; Maddox et al., 1998; Schaufuss et al., 2000). These studies have provided information about elemental oxidation states at the arsenopyrite surface, electrochemical effects, changes in stoichiometry with alteration, and secondary products formed in the absence of bacteria. In doing so, they have improved our understanding of arsenopyrite alteration in air, distilled water, acid, and other oxidizing solutions. To date, however, no studies have used surface analytical techniques, such as X-ray photoelectron spectroscopy (XPS), on arsenopyrite after reaction with iron-oxidizing bacteria, although the reactivity of hematite with sulfate-reducing bacteria has been observed by XPS (Neal et al., 2001). The objective of this study was to observe the chemical and physical changes at a polished

* Author to whom correspondence should be addressed (hwn@uwo.ca).

arsenopyrite surface in the presence of the bacterium *T. ferrooxidans*. The surface changes were analyzed using two complementary techniques: scanning electron microscopy (SEM) and XPS.

2. EXPERIMENTAL METHODS

A time-series experiment was conducted to determine the chemical and physical changes at a polished arsenopyrite surface in the presence of *T. ferrooxidans*. Samples of arsenopyrite were exposed to *T. ferrooxidans* for 1, 2, and 3 weeks. The reacted surfaces were imaged with the scanning electron microscope, and surface chemistry was analyzed with an X-ray photoelectron spectrometer. As a control, arsenopyrite was exposed to bacterial growth medium for the same time periods in the absence of bacteria.

2.1. Sample Preparation and Procedure

The arsenopyrite used in this study was previously collected and individual crystals isolated by L. M. Maddox, University of Western Ontario, London, Canada (Maddox, 1996; Maddox et al., 1998). Polished surfaces were chosen for this study because a fractured surface introduces large irregularities that may cause an XPS depth profile to be difficult to interpret. One face perpendicular to the *c* axis was polished with sequentially finer SiC grit paper and a final polish with 0.25-μm-sized diamond dust. Any residual dust was carefully removed with a dust-free portion of the polishing pad and a Kimwipe. All polishing was dry to keep the arsenopyrite surfaces fresh and uncontaminated by lubricants. The final stage of polishing was in an inert Ar gas atmosphere inside an airtight glove box. The polished crystals were not sterilized by autoclaving or chemical sterilizing agents because of possible surface alteration detectable by the surface-sensitive XPS. It is unlikely that the freshly polished surfaces of arsenopyrite would carry any contaminating bacteria. In addition, the growth medium for *T. ferrooxidans* is unlikely to support growth of potential airborne contaminants, and any contaminating bacteria would be vastly outnumbered by the concentrated suspension of *T. ferrooxidans*. Two polished arsenopyrite crystals were used in each of the bacterial and control treatments for each time period, one for analysis by XPS and one for SEM.

T. ferrooxidans strain DSM 583 was kindly supplied by R. C. Blake II (Xavier University of Louisiana, New Orleans). This strain has been maintained on arsenopyrite for 14 yr and adheres with much greater affinity to arsenopyrite than do other strains of *T. ferrooxidans* (Sampson and Blake, 1999). Strain DSM 583 can be grown on either ferrous sulfate or arsenopyrite and oxidizes Fe^{2+} to Fe^{3+}. Before the experiment, cells were grown on a ferrous sulfate medium identical to that used by Sampson and Blake (1999). This medium contained standard constituents designed to optimize the growth of *T. ferrooxidans* and is described as follows. Distilled deionized water was acidified to pH 2.3 with H_2SO_4. $FeSO_4{\cdot}7H_2O$ was dissolved in the acidified water to a concentration of 0.2 mol/L (or 55.6 g/L), and the pH was readjusted to 2.3. The solution was filter sterilized through a pore size of 0.2 μm and dispensed into sterile, plugged Erlenmeyer flasks. A solution of essential salts (essential for growth) acidified to pH 2.3, autoclaved, and stored in concentrated form (100×) was added aseptically to the ferrous sulfate solution, giving a final concentration of 0.44 g/L each of $MgSO_4{\cdot}7H_2O$ and $(NH_4)_2SO_4$, and 0.11 g/L each of KH_2PO_4 and KCl. Each culture was inoculated with a 5% inoculum by volume of *T. ferrooxidans* and incubated for 5 d at room temperature on a rotary shaker.

After incubation, the cells were isolated from the ferrous sulfate medium using the procedure of Sampson and Blake (1999) for subsequent use in the arsenopyrite experiment. The ferrous sulfate–grown *T. ferrooxidans* culture was filtered through a sterile Whatman #1 filter paper to remove most of the oxidized iron precipitate in suspension. The filtered bacterial suspension was centrifuged at 10,780 g for 30 min in sterile centrifuge tubes. The cells were washed three times in sterile H_2SO_4 (pH 2.3) to minimize the dissolved iron introduced into the experiment, thus ensuring that arsenopyrite was the only energy source available for the cells and that the arsenopyrite was not initially oxidized by Fe^{3+} in solution.

Isolated cells were resuspended in the sterile solution of essential salts at pH 2.3, but without ferrous sulfate. The cells were concentrated in the resuspension to an optical density at 600 nm (OD_{600}) of ~0.3 (5 times their original concentration in the ferrous sulfate culture) to ensure sufficient cells for attachment and reaction with the arsenopyrite. Experiments began concurrently to ensure identical initial optical densities, solution chemistry, and temperature. Three sterile, plugged, 10-mL Erlenmeyer flasks received 5 mL of essential salt solution with suspended *T. ferrooxidans* cells, and three received 5 mL of essential salt solution of identical chemistry with no bacteria. The flasks were placed in an Ar-filled, airtight glove box in which the arsenopyrite laths received their final polish and were added to the flasks. The flasks were incubated on a rotary shaker at room temperature for 1, 2, and 3 weeks, after which the reacted arsenopyrite samples were prepared for analysis.

Samples for SEM study were fixed in glutaraldehyde to maintain cell structure and to secure attached cells to the arsenopyrite surface. Samples were immersed overnight in 2% glutaraldehyde in a 0.1-mol/L sodium cacodylate buffer (CAC) at pH 7.4, rinsed in a CAC buffer, and postfixed for 1 h with 1% OsO_4 in 0.1-mol/L CAC at 4°C. Samples were then dehydrated sequentially in graded ethanol solutions, 50, 70, 85, 95, and 100% EtOH. The arsenopyrite samples with fixed cells were dried using a critical point drier and stored in a desiccator before SEM analysis. They were not gold coated. Samples for analysis by XPS were not fixed, to prevent surface chemical changes. Arsenopyrite with attached bacteria was allowed to dry in an Ar atmosphere and transferred to the X-ray photoelectron spectrometer in a sealed, Ar-filled vessel.

2.2. Instrumentation

Optical density of bacterial cultures was measured with a Philips PYE UNICAM PU8600 UV/Vis spectrophotometer. Each measurement was standardized to deionized, distilled water for zero optical density. The bulk composition of polished sections of arsenopyrite was obtained by electron microprobe analysis using a JEOL JXA-8600 Superprobe (University of Western Ontario). The analyses were conducted using an accelerating voltage of 25 keV and a probe current of 30 nA. X-ray peaks collected were Fe Kα, As Lα, Co Kα, Ni Kα, and S Kα. Co Kα counts were corrected for the slight overlap of the Fe Kβ peak. Counts were integrated for Fe, As, and S for 20 s, and Co and Ni for 30 s. Fe, As, and S were standardized with arsenopyrite, Co with pure cobalt, and Ni with NiS. ZAF matrix corrections were used (i.e., Z for atomic number, A for X-ray absorption and F for X-ray fluorescence). The minimum detection limits in weight percentage were 0.017 for Fe, 0.016 for Co and Ni, 0.045 for As, and 0.011 for S.

SEM images of reacted arsenopyrite were collected with a Hitachi model S-4500 field emission scanning electron microscope at Surface Science Western Laboratories (University of Western Ontario). A beam potential of 5 kV was used. Energy-dispersive X-ray (EDX) analyses were acquired with the same instrument using an EDAX Phoenix model light element detector and the manufacturer's standardless quantification program.

Reacted samples of arsenopyrite were analyzed with an SSX-100 X-ray photoelectron spectrometer with a monochromatized Al Kα X-ray source (1486.6 eV) at Surface Science Western Laboratories. The instrument was standardized to give a value of 84.00 eV for the Au $4f_{7/2}$ line of a gold foil standard. The spectrometer was calibrated so that the energy difference between the Cu $2p_{3/2}$ and Cu $3p_{3/2}$ lines of copper metal was 857.5 ± 0.1 eV. The analytical chamber base pressure was on the order of 10^{-8} torr.

Broad scans (0 to 1000 eV) were collected to identify the range and relative abundance of elements present (Scofield, 1976) using an X-ray beam focused to a spot size of 600 μm and an analyzer pass energy of 150 eV. Depth profiles were collected by alternately analyzing the surface and sputtering with an ion beam of Ar^+. For analysis during profiling, the X-ray beam was focused to a spot size of 600 μm, and an analyzer pass energy of 150 eV was used.

Surface sputtering between each cycle of analysis used an ion energy of 2 kV and an emission current of 10 mA, and the sample was at 30° to the ion beam. Depth (nm) was calculated from sputter time (s) using the erosion rate (nm/s) calculated with the following equation: erosion rate = (%FeAsS)(FeAsS erosion rate) + (%FePO4)(FePO4 erosion

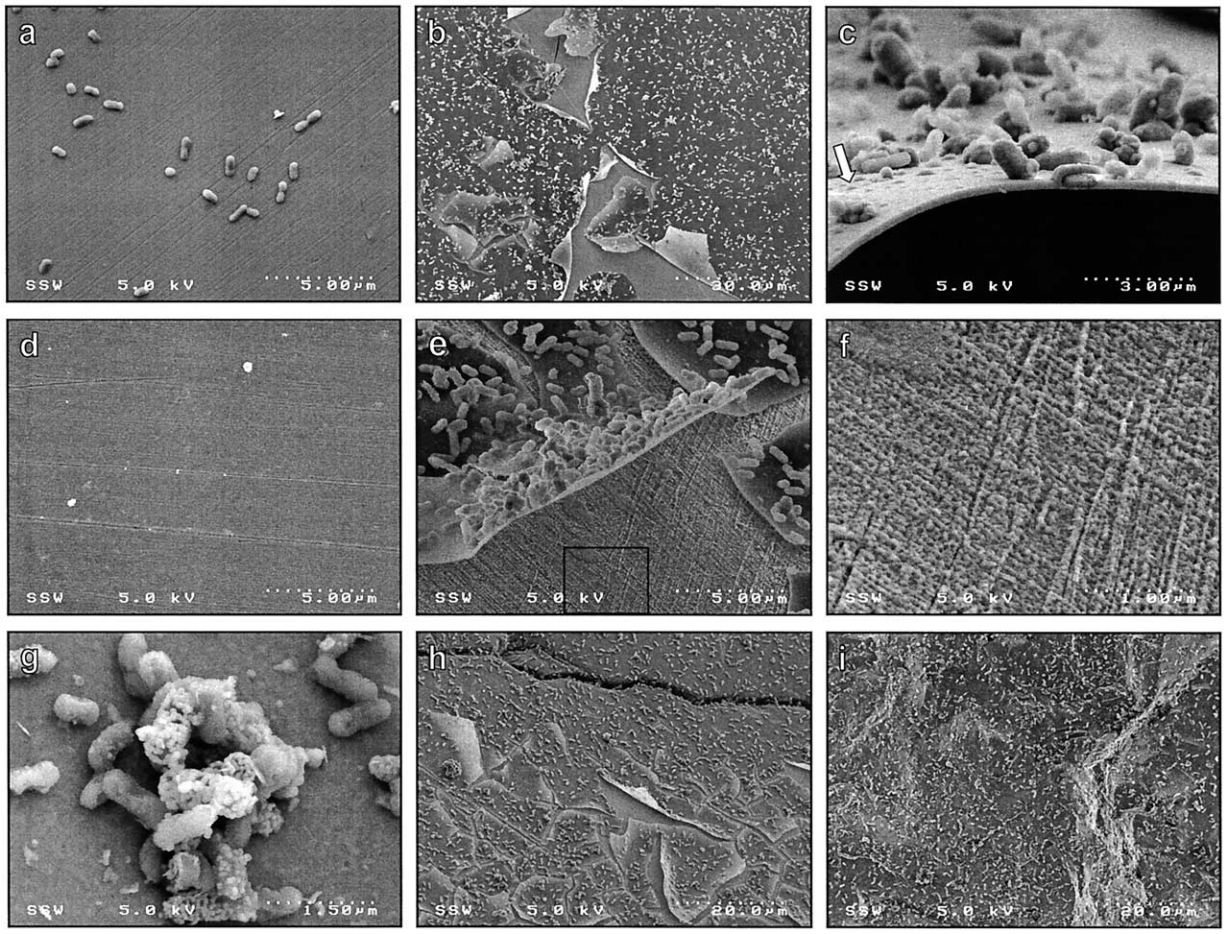

Fig. 1. Scanning electron micrographs of arsenopyrite surfaces. (a) *Thiobacillus ferrooxidans* attached to arsenopyrite after 2 d. The surface has polishing scratches and appears unaltered. (b) Arsenopyrite exposed to *T. ferrooxidans* for 1 week. Cells are attached only to the dehydrated and partially spalled overlayer. (c) The overlayer has a uniform thickness of 240 nm after 1 week. The arrow points to small structures on the surface of the overlayer that may be membrane vesicles released by *T. ferrooxidans*. (d) A surface of arsenopyrite exposed for 2 weeks to the control medium. (e) Arsenopyrite exposed to *T. ferrooxidans* for 2 weeks. The box is magnified in (f). (f) High-magnification image showing the etched appearance of the arsenopyrite surface, with roughly linear intersecting pits, after 2 weeks of exposure to *T. ferrooxidans*. (g) A microcolony of cells after 3 weeks of reaction with arsenopyrite. Some cells remained smooth, and some developed rounded surface structures. (h) Arsenopyrite exposed to *T. ferrooxidans* for 3 weeks. (i) Coarsely polished surface of the same sample of arsenopyrite as in (h). No spalling was observed and cracks were rare, indicating that the undulating surface allowed the overlayer to contract during dehydration while remaining intact.

rate). The erosion rate of arsenopyrite was approximated with that of pyrrhotite (Pratt et al., 1994), which has a similar density, and the erosion rate of $FePO_4$ was calculated from its thickness after 1 week and the sputter time at the boundary between $FePO_4$ and arsenopyrite. The boundary was taken at 50% FeAsS, which was estimated by percentage of S because sulfur is the slowest element to oxidize in arsenopyrite (Buckley and Walker, 1988; Nesbitt et al., 1995; Nesbitt and Muir, 1998) and is less mobile than iron and arsenic.

3. RESULTS AND INTERPRETATION

3.1. Electron Probe Microanalyses of Arsenopyrite

Electron probe microanalysis (EPMA) of arsenopyrite yielded an average (n = 16) composition of $Fe_{0.99}Co_{0.01}As_{0.96}S_{1.08}$, indicating a small amount of substitution of S for As compared to the idealized formula (FeAsS). One standard deviation was 0.002 for Fe, 0.003 for As and S, and ranged between 0.05 and 0.23 for Co. The variability of the standard deviation for Co and its high value relative to other elements indicates that it may be present in trace quantities.

3.2. Arsenopyrite Surface Morphology and Attachment of Bacteria (SEM)

3.2.1. Attachment Test and Abiotic Control

Before the 3-week experiment, cells grown on ferrous sulfate were exposed to polished arsenopyrite for 2 d to determine if they would attach. SEM images of the arsenopyrite surface after exposure to *T. ferrooxidans* for 2 d revealed that some cells did attach but were sparsely distributed (Fig. 1a). The arsenopyrite surface appeared unaltered, and polishing scratches were visible.

Over the entire 3-week period, arsenopyrite exposed to the growth medium in the absence of bacteria was visually unaltered from a freshly polished surface. It was smooth, with only a few polishing scratches visible. Figure 1d gives a representative image of the abiotic arsenopyrite surface after 2 weeks.

3.2.2. Arsenopyrite Surface With T. ferrooxidans

After 1 week, an overlayer had developed on the arsenopyrite surface (Fig. 1b). Its absence in the 2-d experiment constrains its formation to between 2 and 7 d. The overlayer cracked and spalled from the surface during dehydration or under the vacuum of the scanning electron microscope. EDX analysis of the overlayer revealed Fe, As, and S, with trace amounts of P and O. The overlayer was highly uniform (Fig. 1c). Thickness of the overlayer after each reaction period was measured to be between 0.1 and 0.25 μm.

After 2 and 3 weeks (Figs. 1e and 1h), the overlayer appeared similar to the 1-week sample, but the underlying arsenopyrite surface had developed an irregular, etched texture, with two sets of roughly linear intersecting features (Fig. 1f). These features may be coalesced etch pits formed along dislocations (Pratt et al., 1994) or along polishing scratches. The increased corrosion beneath the overlayer suggests that the overlayer did not act as a barrier to reaction.

Figures 1h and 1i display two different surfaces of the same sample of arsenopyrite exposed to *T. ferrooxidans* for 3 weeks. The flat surface in Figure 1h was finely polished before exposure, as were all the other surfaces analyzed by XPS and SEM, but the surface in Figure 1i was only coarsely polished and displays some surface topography. No spalling was observed on the latter surface, and cracks were very rare. The undulating surface may have been more forgiving to expansion or contraction, allowing the overlayer to contract during dehydration and remain intact. This suggests that on a fractured surface, as would occur during milling or in laboratory experiments using powdered sample, an overlayer would be extremely difficult to observe and may escape detection without surface-sensitive chemical analysis. The lack of spalling in Figure 1i also lends supporting evidence for continuous coverage of the overlayer overall arsenopyrite surfaces while in solution before dehydration and sample analysis.

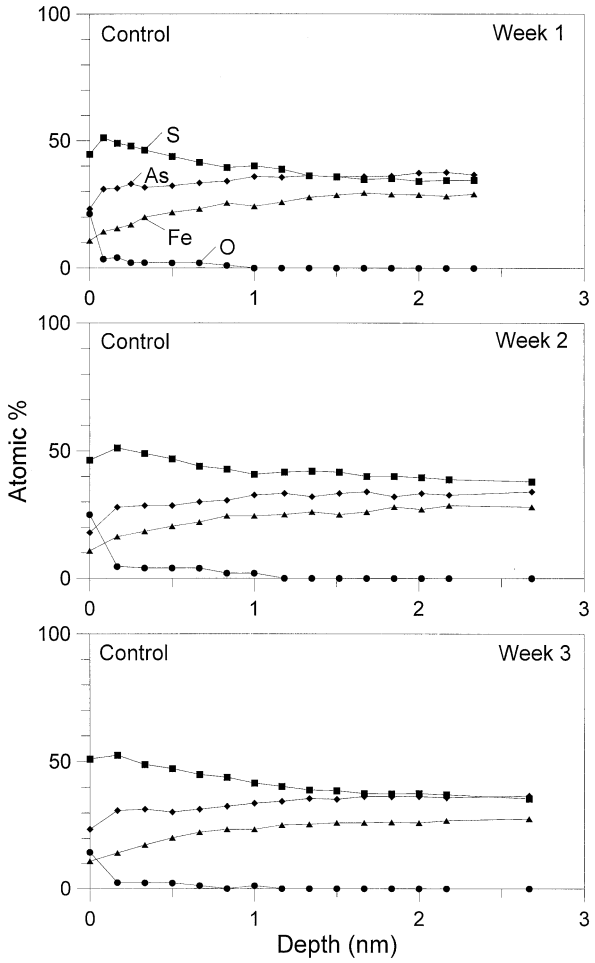

Fig. 2. X-ray photoelectron spectroscopy depth profiles of arsenopyrite exposed to the control solution for 1, 2, and 3 weeks. Atomic percentage and depth were calculated from spectral peak area and sputter time. Elements shown are O = ●, Fe = ▲, As = ◆ and S = ■. Surface alteration was thin, increasing between 1 and 2 nm over 1, 2, and 3 weeks. Alteration consists of a slight S enrichment and corresponding depletion of Fe and As, indicating dissolution of the latter two elements. Trace O was detected at the surface, indicating slight oxidation.

3.2.3. Distribution of T. ferrooxidans

The arsenopyrite surface after 1 week of reaction exhibited more attached cells than the 2-d test sample (compare Figs. 1a and 1b), whereas the 2- and 3-week samples (Figs. 1e and 1h) displayed similar bacterial distributions to the 1-week sample. The cells were attached to the overlayer, not the arsenopyrite. This indicates that the overlayer was intact in the cell suspension and cracked only after the sample was removed from the experiment. Thus, after only 1 week of reaction, the cells were completely isolated from the arsenopyrite by the overlayer.

3.2.4. Bacterial and Overlayer Surface Morphology

Some cells exhibited rounded surface structures that varied in size but were ~0.5 μm in diameter (Fig. 1g). These structures were seen on some cells after 1, 2, and 3 weeks, but not on any cells after 2 d. In addition, small vesicles or blebs were observed on the overlayer (Fig. 1c). These were not associated with the bacterial cells. These structures may be analogous to outer-membrane vesicles, which can be released by various gram-negative bacteria (such as *T. ferrooxidans*) during growth (Beveridge, 1999). Interestingly, this has been found to be important during biooxidation of S^0 by *T. thiooxidans* (Knickerbocker et al., 2000).

3.3. XPS Compositional Depth Profiles of Arsenopyrite

3.3.1. Abiotic Control

XPS depth profiles of the arsenopyrite surface exposed only to the solution of essential salts revealed very little alteration over the 3-week period (Fig. 2). Only trace oxygen was detected at the surface, and this disappeared at a depth of ~1 nm, indicating slight oxidation. The surface was slightly enriched in

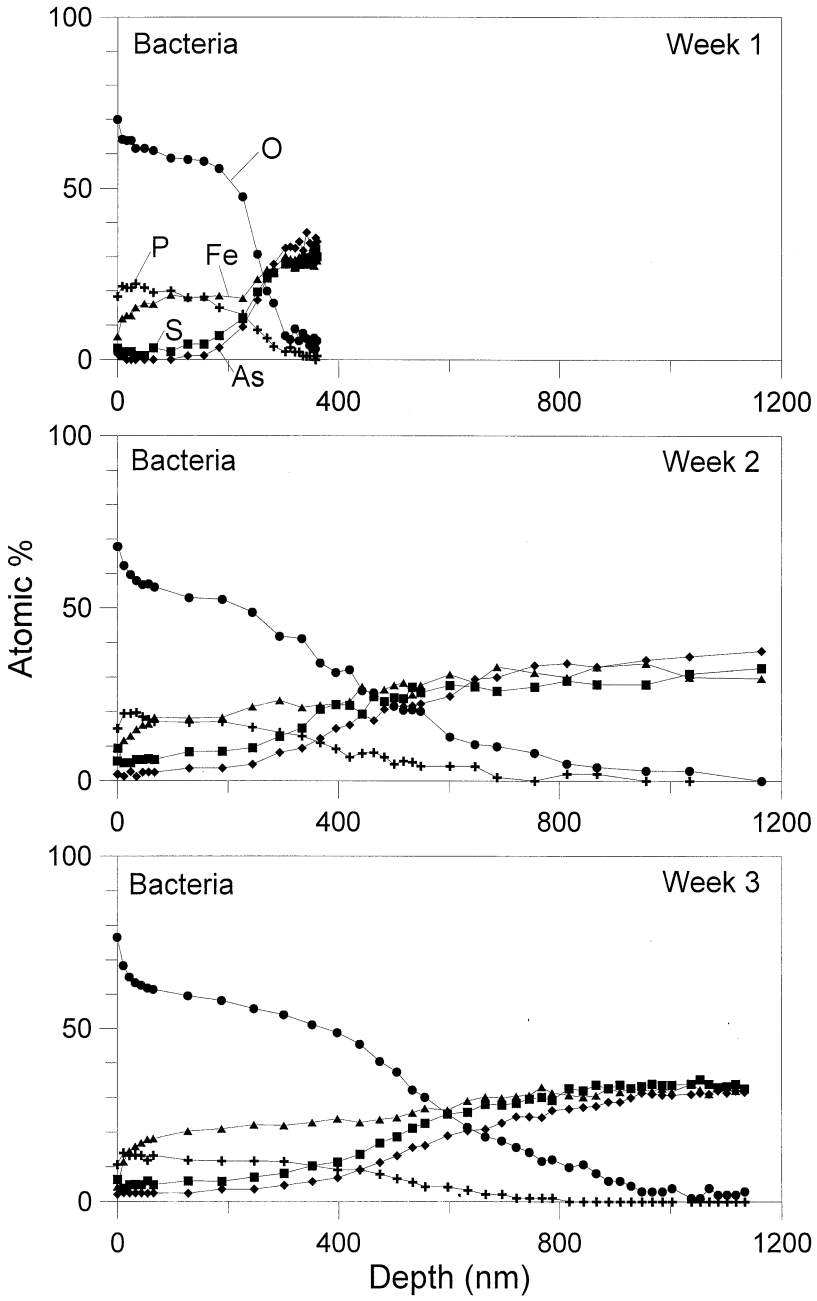

Fig. 3. X-ray photoelectron spectroscopy depth profiles of arsenopyrite (FeAsS) exposed to *Thiobacillus ferrooxidans* for 1, 2, and 3 weeks. Atomic percentage and depth were calculated from spectral peak area and sputter time. Elements shown are O = ●, P = +, Fe = ▲, As = ◆, and S = ■. Surface alteration was orders of magnitude thicker than the control. Surface composition exhibited equal proportions of Fe and P and roughly 4 times as much O. This indicates that the overlayer observed in scanning electron microscopy images was composed of $FePO_4$. As and S were not present at the surface but increased in concentration with depth as O and P decreased. After 1 week of reaction, Fe, As, and S were present in equal proportions at a depth of ~300 nm, indicating fresh arsenopyrite. Over 2 and 3 weeks, the boundary between $FePO_4$ and FeAsS extended deeper and became more gradual, indicating continued oxidation and diffusion.

sulfur and correspondingly depleted in arsenic and iron, indicating dissolution of the latter two elements (Nesbitt et al., 1995). Because there was no S-depleted region below the S-rich surface, one may rule out preferential diffusion of S to the surface. Only the surface-most 1.3 to 1.7 nm were altered between 1 and 3 weeks (Fig. 2).

3.3.2. Arsenopyrite Surface With T. ferrooxidans

The XPS depth profile of arsenopyrite exposed to *T. ferrooxidans* for 1 week (Fig. 3) showed that alteration extended 2 to 3 orders of magnitude deeper than the sample exposed to the control solution. The composition of the surface exhibited

equal proportions of iron and phosphorus and roughly 4 times as much oxygen. This indicates that the surface overlayer observed in the SEM images was composed of iron phosphate ($FePO_4$). The iron phosphate was likely hydrated (because it formed in aqueous solution) and may be the mineral strengite ($FePO_4 \cdot 2H_2O$). Precipitation of strengite from iron- and phosphate-rich solutions in nature has been noted previously (Ehrlich, 1996, and references therein). Arsenic and sulfur were not present on the surface but increased in concentration with depth (between 150 and 300 nm) as oxygen and phosphorus decreased. At a depth of ~300 nm, iron, arsenic, and sulfur were present in equal proportions. This indicates fresh arsenopyrite (FeAsS).

After 2 weeks (Fig. 3), the $FePO_4$ overlayer thickened, and the compositional transition to fresh arsenopyrite was deeper and more gradual (~200 to 800 nm). After 3 weeks, the $FePO_4$ overlayer was roughly 3 times thicker than after 1 week of reaction. The transition to fresh arsenopyrite extended between 300 and 1000 nm (Fig. 3). Clearly, the arsenopyrite continued to alter beneath the $FePO_4$ overlayer. The gradual change in composition indicates diffusion, the deeper penetration of oxygen indicates oxidation, and the increasing roughness observed by SEM indicates dissolution.

Figure 4 displays the stacked spectra from the altered surface ($FePO_4$) to fresh arsenopyrite (FeAsS) at depth, after 1 week of reaction. The Fe 3p spectra show a shift in binding energy from ≥55 eV at the surface to between 53 and 54 eV at depth. This indicates that iron was oxidized (Fe^{3+}) in $FePO_4$ and reduced (Fe^{2+}) in arsenopyrite. Although Tsang et al. (1979) noted that iron-sulfur compounds may be reduced by ion bombardment, the presence of Fe^{3+} in the stacked iron spectra (Fig. 4) indicates that sputtering did not reduce Fe^{3+} in these samples. Sputtering also increases surface roughness and may force surface atoms deeper than they were originally, causing compositional gradients to appear more gradual (Pratt et al., 1994, and references therein). Although the transition zone between $FePO_4$ and FeAsS may appear more gradual in Figures 3 and 4 than the actual boundary, the relationships among elements are still clear. The As 3d and S 2p spectra exhibit peaks only at depth, at 41.5 and 62.5 eV, respectively. These peaks gradually disappear toward the surface. Conversely, the P 2p and O 1s spectra exhibit peaks only at the surface (near 134 and 531.7 eV) that disappear at depth. The P 2p spectral window also shows an As Auger peak between 140 and 141 eV that disappears as the P 2p peak appears. This clearly shows that As and P have an inverse relationship and that the zone of chemical transition coincides.

The C 1s stacked spectra of Figure 4 illustrate the distribution and nature of the carbon species in the $FePO_4$ overlayer. The most intense carbon signal was obtained at the solution-$FePO_4$ interface (labeled "surface" in Fig. 4). The signal is characterized by a peak maximum at 285 eV, indicative of adventitious carbon (hydrocarbons derived from vacuum pump oils are ubiquitous as residual gases in the vacuum of the analytical chamber). The high–binding energy tail extending to ~290 eV signifies the presence of organic carbon of organic molecules. Carbon of carboxylic groups, for example, contribute to the spectrum between ~287 and 290 eV (Stipp and Hochella, 1992; Banerjee and Nesbitt, 1999, and references therein). Signal intensity between ~286 and 290 eV decreases to zero after ~10 sputtering cycles (10th scan line from surface in Fig. 4, C 1s spectrum). This demonstrates the absence of organic carbon and organic species at depth beyond the 10th scan.

The $FePO_4$-FeAsS interface is much deeper than this and is first detected after ~40 sputtering cycles (Fig. 4, As 3d spectrum). Therefore, no organic species are present at the arsenopyrite surface where it undergoes dissolution, regardless of what organic species are present in the bulk solution. Because they are absent, organic species cannot be involved in the dissolution mechanism at the arsenopyrite surface. It must be concluded that oxidative dissolution of arsenopyrite below the $FePO_4$ overlayer is purely an inorganically controlled reaction, mediated by bacterial activity.

4. DISCUSSION AND CONCLUSIONS

4.1. Initial Formation of the $FePO_4$ Overlayer

In this study, iron used in $FePO_4$ formation must have come from the arsenopyrite, because no iron was added to the solution of essential salts. The lack of $FePO_4$ on the control sample indicates that *T. ferrooxidans* must be responsible in some way for its formation. However, the uniformity in thickness and lateral continuity of the overlayer indicates an inorganic process. If *T. ferrooxidans* were directly involved in precipitation of $FePO_4$, one would expect the overlayer to be localized near each cell or group of cells, perhaps with regions of the surface where $FePO_4$ was thinner or absent where bacteria were not represented. *T. ferrooxidans* must have promoted the formation of the overlayer through the oxidation of Fe^{2+} to Fe^{3+}, which was released to solution and precipitated with PO_4^{3-} from the medium (Fig. 5).

4.2. Possible Origin of Cell Surface Structures

The composition and origin of the rounded structures on some *T. ferrooxidans* surfaces (Fig. 1g) are uncertain. They may be membrane vesicles still attached to the cell surface, as described by Beveridge (1999). Alternatively, the structures may have precipitated from solution at the cell surface. The composition of the surface structures was not determined, because of interference from the strong arsenopyrite signal during EDX analysis, but $FePO_4$ or iron oxide are candidates. Fortin et al. (1996) observed numerous mineralized bacteria from mine tailings, many with amorphous iron oxides on their cell walls. Southam and Beveridge (1992) examined thin sections of thiobacilli from the Lemoine mine tailings (Chibougamau, Quebec, Canada) and identified some spherical structures on the cell surface as an iron phosphate. Konhauser et al. (1994) observed complete encrustation of some bacterial cells by iron phosphates that were similar to the mineral strengite ($FePO_4 \cdot 2H_2O$). These cells were within a microbial biofilm on Ellesmere Island.

Nordstrom and Southam (1997) presented a model of iron oxidation by *T. ferrooxidans* involving the intake of Fe^{2+} and the release of Fe^{3+} through pores at the cell surface. Perhaps $FePO_4$ formed at the cell surface surrounding these pores as the released Fe^{3+} reacted with the PO_4^{3-} in solution to precipitate an $FePO_4$ salt (Fig. 6).

If the rounded surface structures are $FePO_4$, their presence on some cells and not others may reflect metabolic activity. Bacterial metabolism may encourage $FePO_4$ deposition in two

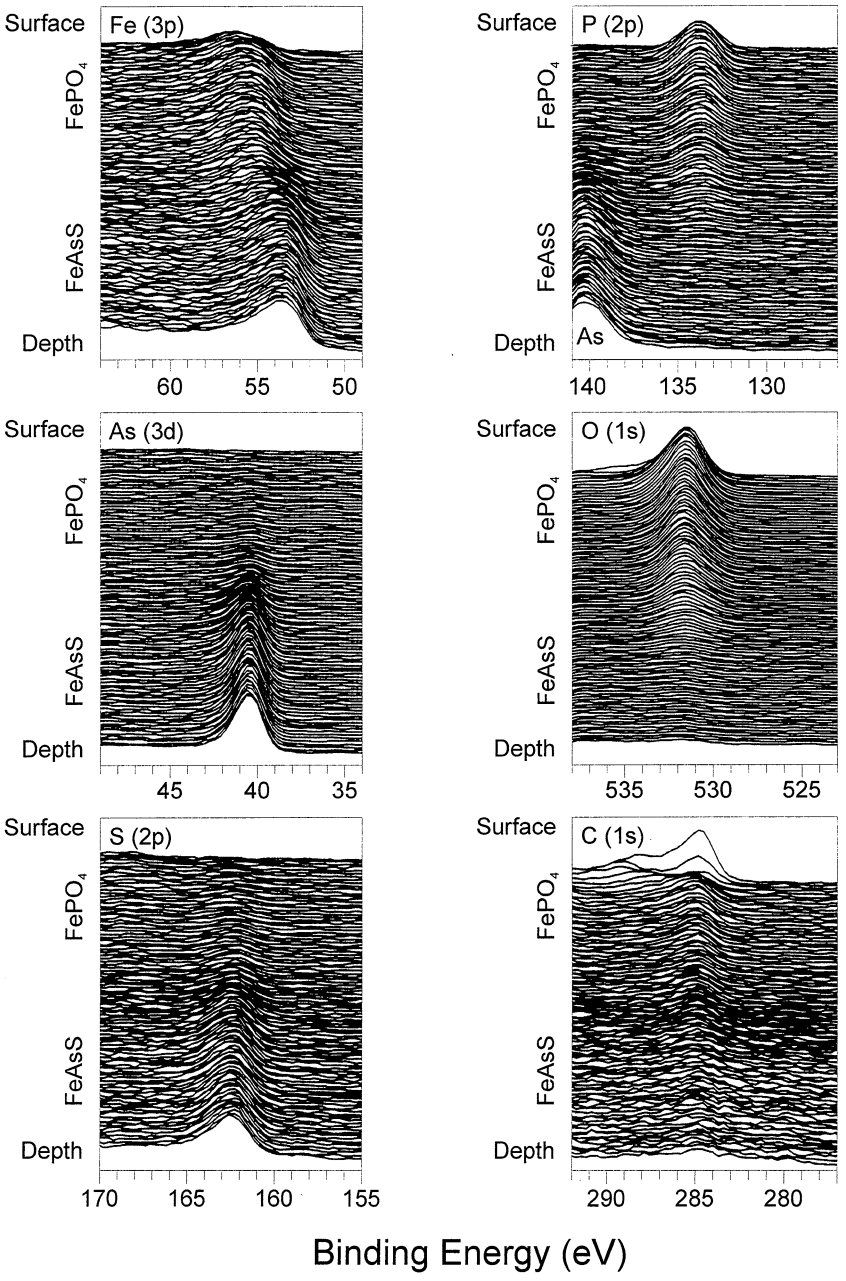

Fig. 4. Spectral display of a depth profile through the surface of arsenopyrite (FeAsS) exposed to *Thiobacillus ferrooxidans* for 1 week. Peak intensity (photoelectron counts, in arbitrary units) is plotted on the *y* axis and binding energy on the *x* axis. Each binding energy window shows an element peak changing in intensity or binding energy with depth through the $FePO_4$ overlayer at the surface to fresh FeAsS at depth. The peak near 140 eV in the P (2p) spectrum corresponds to an As Auger peak.

ways: (1) by liberating Fe^{3+} to solution and (2) by the consumption of H^+ in the cell interior via oxygen reduction to produce water. The latter may basify the region immediately surrounding the cell relative to the bulk of solution. Basification could promote the dissociation of KH_2PO_4, which liberates the PO_4^{3-} anion to precipitate with Fe^{3+}.

If cells were collected from solution, the elemental composition of the rounded surface structures could be determined by EDX analysis in the scanning electron microscope without interference from the strong arsenopyrite signal. Alternatively, EDX analysis by transmission electron microscopy could identify the surface structures because of the finer spot size.

4.3. Alteration of Arsenopyrite in the Presence of the $FePO_4$ Overlayer

There is an ongoing debate concerning the mechanism of alteration of metal sulfides by bacteria, as discussed in a num-

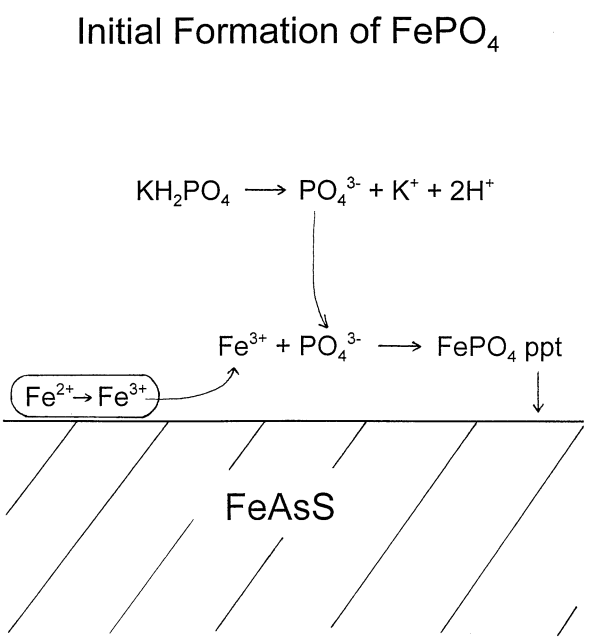

Fig. 5. Schematic diagram of the initial formation of the $FePO_4$ overlayer.

ber of recent reviews (Sand et al., 1995; Nordstrom and Southam, 1997; Ehrlich, 1997, 1998). The direct biologic mechanism involves direct contact between a mineral surface and a cell that actively instigates mineral oxidation and leaching. The indirect mechanism is in fact an inorganic mechanism that involves the oxidation of a mineral by Fe^{3+}. The source of the Fe^{3+}(aq) is immaterial to the reaction mechanism and may include Fe^{3+}(aq) released from cells as a waste product. Release of Fe^{3+} and its migration to the arsenopyrite surface will result in transfer of an electron from the mineral to Fe^{3+} adsorbed to the surface (McKibben and Barnes, 1986; Luther, 1987). This mechanism is strictly inorganic, with the bacteria supplying reactant. Once the surface iron is reduced, it is then available as an electron source for the bacteria. In this way, arsenopyrite is oxidized, and the bacteria maintain a supply of electrons required for energy production (Nordstrom and Southam, 1997).

In this study, there is no doubt that arsenopyrite beneath the $FePO_4$ overlayer continued to react over 2 and 3 weeks, as evidenced by more extensive alteration observed by XPS and textural changes in SEM images. After 1 week, *T. ferrooxidans* was isolated from the arsenopyrite surface by the uniform overlayer. Arsenopyrite alteration must, however, still have been assisted by bacteria, because over the 3-week period, the XPS depth profiles of the abiotic control showed orders of magnitude less alteration. Two conclusions are indicated by these results: Bacteria need not be attached to arsenopyrite to promote rapid reaction, and the reaction mechanism in this case must have been inorganic but promoted by bacterial action. Some authors have concluded that bacteria must be directly attached to be able to leach a mineral surface (Arredondo et al., 1994; Sand et al., 1995). For this study, attachment was unnecessary to enhance arsenopyrite dissolution.

4.4. Implications for Remediation by $FePO_4$ Coatings

Evangelou (1994) suggested a remediation method involving $FePO_4$ to prevent acidic drainage in mine tailings from the oxidation of sulfides. The study investigated the formation of an $FePO_4$ coating and its effectiveness as a barrier to oxidation. Powdered pyrite was oxidized with H_2O_2 to release Fe^{3+} that reacted with KH_2PO_4 in solution. Evangelou (1994) concluded that the $FePO_4$ coating on pyrite effectively protected it from oxidizing further in two ways: (1) by providing an iron sink for Fe^{3+} (preventing it from oxidizing pyrite) and (2) by forming a passive coating. A plot of percentage pyrite remaining vs. time clearly displayed the observed inhibiting effect of the coating compared to uncoated pyrite (Evangelou, 1994) and showed that the $FePO_4$ coating slowed oxidation. Evangelou (1994) concluded that the prevention of acid mine drainage could be permanent with an $FePO_4$ coating.

Unfortunately, $FePO_4$ may not be as effective a barrier to oxidation in the tailings environment as Evangelou (1994) suggested. The overlayer observed in this study appears permeable and delicate, easily cracked and spalled by dehydration. This is an important consideration in an alternately wet and dry environment. To maintain the structural integrity of the coating, it would have to be permanently submerged in an aqueous environment to prevent dehydration cracking. If the layer remains intact, it offers a retarding effect on oxidation reactions (Evangelou, 1994) because diffusion of oxygen and Fe^{3+} through the $FePO_4$ layer are likely slower than through solution. However, this study has shown that diffusion does occur, and arsenopyrite continues to react beneath the overlayer over the interval of 3 weeks. The $FePO_4$ thickness of Evangelou (1994) was estimated at 18.8 nm, whereas in this study, it was 200 nm thick after 1 week of reaction. Even so, the arsenopyrite below the thicker overlayer continued to react. Evangelou (1994) concluded that an $FePO_4$ coating was an effective inhibitor of H_2O_2. Perhaps molecular oxygen or Fe^{3+} diffuses more easily through $FePO_4$. The results presented here indicate that oxidation and dissolution proceed rapidly when promoted by bacteria, even in the presence of an $FePO_4$ overlayer.

A further concern is that the addition of PO_4^{3-} to a sulfide-rich area may only encourage growth of sulfide-oxidizing bacteria by providing an essential nutrient that is growth limiting in many environments. If a different anion than PO_4^{3-} could be found to form an equally insoluble product with oxidized iron, one that would not provide nutrients to bacteria, its effectiveness as a barrier to oxidation would be worth studying.

4.5. Implications for Laboratory Experiments on Sulfide Oxidation by *Thiobacillus*

The most important conclusion of this study is that the $FePO_4$ coating resulted from iron-sulfide oxidation in a phosphate-rich medium designed to optimize the growth of *T. ferrooxidans*. Phosphate-rich media have been used in numerous experiments on the effect of *T. ferrooxidans* on powdered sulfide minerals. Previous experiments have analyzed solution chemistry or bulk secondary products, but not the composition of the sulfide surface. An overlayer such as this likely cannot be detected by SEM or EDX until it reaches micrometer-scale thickness. It almost certainly has formed but has gone unde-

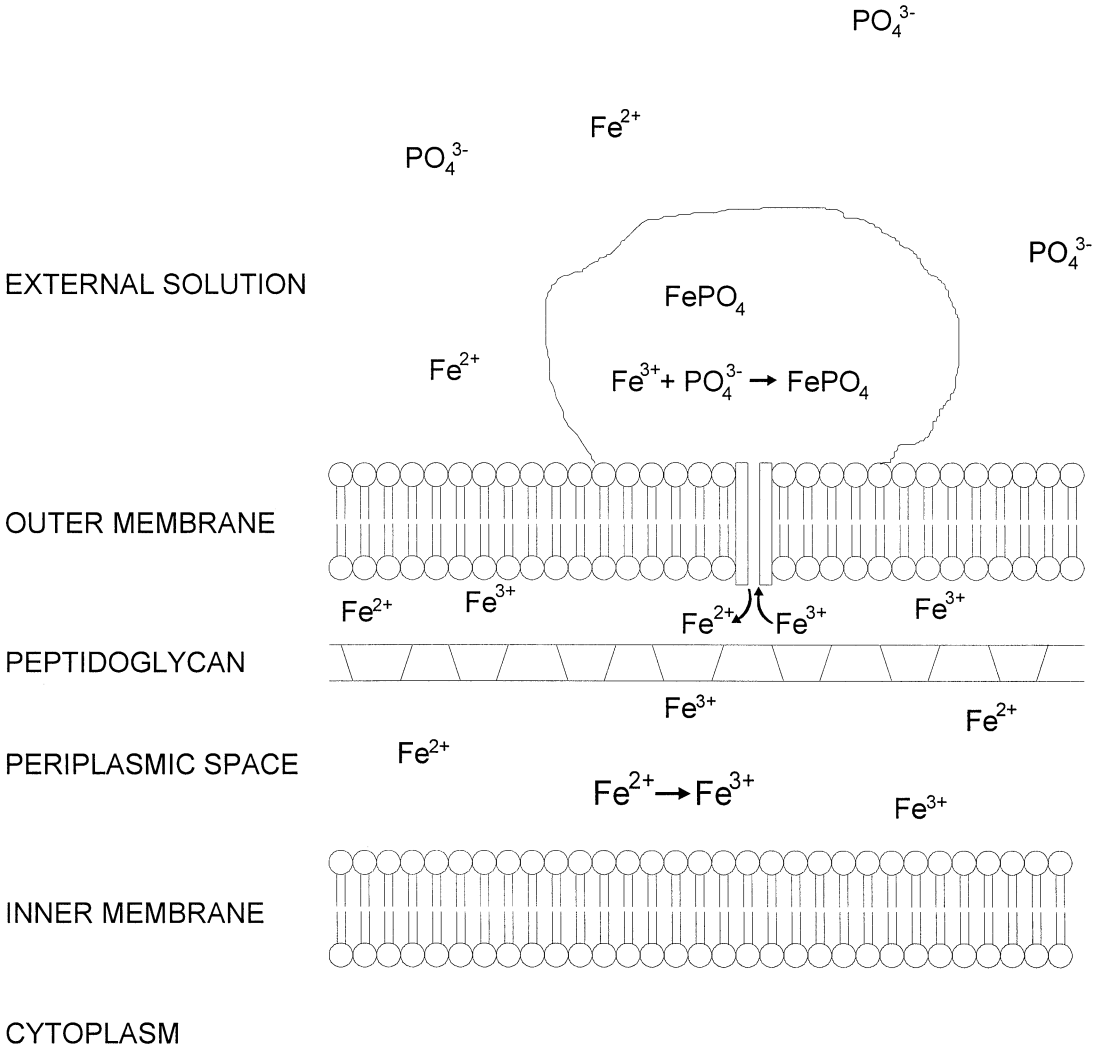

Fig. 6. Schematic cross-section through a portion of the surface of *Thiobacillus ferrooxidans*. A pore in the outer membrane allows the exchange of Fe^{2+} and Fe^{3+}, and iron is oxidized in the periplasmic space by a metabolic process (modified from Ingledew et al., 1977; Blake et al., 1992; Nordstrom and Southam, 1997). Peptidoglycan is the rigid layer of the cell wall. The oxidized iron is released as a waste product through the outer membrane pore, where it may come in contact with PO_4^{3-} ions in solution and precipitate at the cell surface. This is a possible origin for the rounded surface structures observed covering cells after reaction with arsenopyrite for 1, 2, and 3 weeks.

tected in other experiments. Thus, misinterpretation of the reactions occurring during bacterially assisted sulfide oxidation is possible because the effect of diffusion through a coating on reaction rates has not been accounted for. Also, iron in solution may be anomalously low after precipitation with phosphate, which may affect the oxidation rate indirectly. In addition, most natural conditions have much lower phosphate concentrations. Thus, any study using a phosphate-rich medium may be misleading to our understanding of the reactions occurring between *Thiobacillus* and sulfides in nature.

Past research supports this conclusion. A review article on the microbial leaching of sulfide ores by *T. ferrooxidans* stated that "phosphate occurs in natural waters in very low concentrations. . .in controlled microbiological leaching systems additional phosphate may interfere with contact between bacteria and ore particles when it precipitates on the mineral surfaces" (Tuovinen and Kelly, 1972, p. 325). Harahuc et al. (2000a) noted that phosphate concentrations above 25 mmol/L completely inhibited the dissolution of Fe from pyrite and sphalerite by *T. ferrooxidans*. Although Harahuc et al. (2000b) did not observe an $FePO_4$ overlayer, they suggested that phosphate may "bind soluble ferric iron by forming a ferric phosphate precipitate. Iron leaching would then be incorrectly assessed when only the leachate is analyzed" (p. 200). A recent study on the iron reducing bacterium *Shewanella putrefacians* (Zachara et al., 2001) observed the formation of vivianite ($Fe_3[PO_4]_2 \cdot 8H_2O$) crystals (5 to 30 μm long) at the surface of goethite (α-FeOOH). The vivianite crystals formed in all treatments in which PO_4^{3-} was added to the growth medium. This supports the conclusion that iron phosphate minerals are likely to precipitate in laboratory experiments containing high phosphate growth media. In addition, Evangelou (1994) observed

that leaching pyrite with an oxidizing solution containing H_2O_2 and phosphate will introduce an iron phosphate coating on any size of particles, even smaller than 60 mesh sieve. This indicates that experiments on powdered sulfides, in addition to polished crystals, are likely to develop iron phosphate coatings.

The surface analytical technique used is critical in the detection of the $FePO_4$ coating over arsenopyrite. In this study, it was clearly observed by XPS. Less surface-sensitive techniques may not reveal its presence so obviously. EDX analyses of the coated arsenopyrite in this study detected $<5\%$ phosphorus, a level that might be dismissed as belonging to attached bacteria. SEM image comparison of finely polished and coarsely polished arsenopyrite surfaces also indicated that an overlayer is difficult to observe on an irregular surface when still intact and may escape detection without surface-sensitive chemical analysis.

The average contribution of total phosphorus to fresh water is 0.02 mg/kg (Bowen, 1979; Ehrlich, 1996), or 0.02 mg/L. The initial total phosphorus in solution in our experiments was 25 mg/L, over 3 orders of magnitude higher. Evangelou (1994) observed that an $FePO_4$ coating formed on pyrite abiotically with as low a phosphate concentration as 10^{-4} mol/L (3.1 mg/L phosphorus). If laboratory experiments could be conducted below this concentration, $FePO_4$ precipitation would be less likely to present a problem. *T. ferrooxidans* may have an environmental phosphate scavenging system for low phosphate conditions (Seeger and Jerez, 1992). However, McCready (1986) estimated that a phosphate concentration of 1 to 2×10^{-4} mol/L is required for bacterial leaching. G. Southam (personal communication) observed that *T. ferrooxidans* cannot grow in batch culture at one tenth the phosphate concentration of the standard growth medium. These estimates are 2 orders of magnitude higher than most natural conditions. Perhaps a flow-through experiment would allow *T. ferrooxidans* to grow at lower concentrations of phosphate by approximating the circulation of natural waters. If it would be possible to maintain reasonable cell growth, sulfide oxidation experiments in a medium with phosphate levels closer to the concentration in mine tailings would be informative and might provide more applicable predictions for interactions between *T. ferrooxidans* and sulfide minerals.

Acknowledgments— The authors wish to express their appreciation to R. C. Blake II (Xavier University of Louisiana, New Orleans) for providing a culture of arsenopyrite-adapted *Thiobacillus ferrooxidans* and for valuable advice on culture maintenance. X-ray photoelectron spectra and scanning electron micrographs were collected at the Surface Science Western Laboratories, University of Western Ontario. Special thanks to A. R. Pratt for instruction on the use of the X-ray photoelectron spectrometer. Much appreciation is due to R. Davidson for valuable assistance with XPS depth profiling, SEM analysis, and interpretation of samples. Thanks also to J. Sholdice and H. Leung for their help in sample preparation for SEM and Y. Thibault for assistance with EPMA. Financial support was gratefully received from the Natural Sciences and Engineering Research Council through research grants to H. W. Nesbitt and S. F. Koval and a postgraduate scholarship to R. A. Jones.

Associate editor: J. P. Amend

REFERENCES

Arredondo R., Garcia A., and Jerez C. A. (1994) Partial removal of lipopolysaccharide from *Thiobacillus ferrooxidans* affects its adhesion to solids. *Appl. Environ. Microbiol.* **60,** 2846–2851.

Beveridge T. J. (1999) Structures of gram-negative cell walls and their derived membrane vesicles. *J. Bacteriol.* **181,** 4725–4733.

Blake R. B. II, Shute E. A., Waskovsky J., and Harrison A.P. (1992) Respiratory components in acidophilic bacteria that respire on iron. *Geomicrobiol. J.* **10,** 173–192.

Bowen H. J. M. (1979) *Environmental Chemistry of the Elements*. Academic Press, London.

Buckley A. N. and Walker G. W. (1988) The surface composition of arsenopyrite exposed to oxidizing environments. *Appl. Surf. Sci.* **35,** 227–240.

Collinet M.-N. and Morin D. (1990) Characterization of arsenopyrite oxidizing *Thiobacillus*. Tolerance to arsenite, arsenate, ferrous and ferric iron. *Antonie van Leeuwenhoek* **57,** 237–244.

Ehrlich H. L. (1964) Bacterial oxidation of arsenopyrite and enargite. *Econ. Geol.* **59,** 1306–1312.

Ehrlich H. L. (1996) *Geomicrobiology*. 3rd ed. Marcel Dekker, New York.

Ehrlich H. L. (1997) Microbes and metals. *Appl. Microbiol. Biotechnol.* **48,** 687–692.

Ehrlich H. L. (1998) Geomicrobiology: Its significance for geology. *Earth. Sci. Rev.* **45,** 45–60.

Evangelou V. P. (1994) Potential microencapsulation of pyrite by artificial inducement of $FePO_4$ coatings. In *Proceedings of the International Land Reclamation and Mine Drainage Conference and Third International Conference on the Abatement of Acidic Drainage, Vol. 2: Mine Drainage*. Bureau of Mines Special Publication SP 06B-94, pp. 96–103. United States Department of the Interior, Washington, DC.

Fernandez P. G., Linge H. G., and Wadsley M. W. (1996) Oxidation of arsenopyrite (FeAsS) in acid part I: Reactivity of arsenopyrite. *J. Appl. Electrochem.* **26,** 575–583.

Fortin D., Davis B., and Beveridge T. J. (1996) Role of *Thiobacillus* and sulfate-reducing bacteria in iron biocycling in oxic and acidic mine tailings. *FEMS Microbiol. Ecol.* **21,** 11–24.

Groudeva V. I., Groudev S. N., and Markov K. I. (1986) A comparison between mesophilic and thermophilic bacteria with respect to their ability to leach sulfide minerals . In: *Fundamental and Applied Biohydrometallurgy* (eds. R. W. Lawrence, R. M. R. Branion, and H. G. Ebner), p. 484–485. Elsevier, Amsterdam, the Netherlands.

Harahuc L., Lizama H. M., and Suzuki I. (2000a) Selective inhibition of the oxidation of ferrous iron or sulfur in *Thiobacillus ferrooxidans*. *Appl. Environ. Microbiol.* **66,** 1031–1037.

Harahuc L., Lizama H. M., and Suzuki I. (2000b) Effect of anions on selective dissolution of zinc and copper in bacterial leaching of sulphide ores. *Biotech. Bioeng.* **69,** 196–203.

Ilyaletdinov A. N. and Abdrashitova S. A. (1981) Autotrophic oxidation of arsenic by a culture of *Pseudomonas arsenitoxidans*. *Mikrobiol.* **50,** 197–204.

Ingledew W. J., Cox J. C., and Halling P. J. (1977) A proposed mechanism for energy conservation during Fe^{2+} oxidation by *Thiobacillus ferrooxidans*: Chemiosmotic coupling to net H^+ influx. *FEMS Microbiol. Lett.* **2,** 193–197.

Knickerbocker C., Nordstrom D. K., and Southam G. (2000) The role of "blebbing" in overcoming the hydrophobic barrier during biooxidation of elemental sulfur by *Thiobacillus ferrooxidans*. *Chem. Geol.* **169,** 425–433.

Konhauser K. O., Fyfe W. S., Schultzelam S., Ferris F. G., and Beveridge T. J. (1994) Iron phosphate precipitation by epilithic microbial biofilms in Arctic Canada. *Can. J. Earth Sci.* **31,** 1320–1324.

Luther G. W., III (1987) Pyrite oxidation and reduction: Molecular orbital theory considerations. *Geochim. Cosmochim. Acta* **51,** 3193–3199.

Maddox L. M. (1996) *Electrochemical and Spectroscopic Investigation of Metals Deposited on Sulfide Minerals*. Ph.D. thesis, University of Western Ontario, London, Canada.

Maddox L. M., Bancroft G. M., Scaini M. J., and Lorimer J. W. (1998) Invisible gold: Comparison of Au deposition on pyrite and arsenopyrite. *Am. Mineral.* **83,** 1240–1245.

Mandl M., Matulová P., and Dočekalová H. (1992) Migration of arsenic(III) during bacterial oxidation of arsenopyrite in chalcopyrite concentrate by *Thiobacillus ferrooxidans*. *Appl. Microbiol. Biotechnol.* **38,** 429–431.

McCready R. G. L. (1986) Nutrient requirements for the in-place leaching of uranium by *Thiobacillus ferrooxidans*. *Hydrometallurgy* **17,** 61–71.

McKibben M. A. and Barnes H. L. (1986) Oxidation of pyrite in low temperature acidic solutions: Rate laws and surface textures. *Geochim. Cosmochim. Acta* **50,** 1509–1520.

Neal A. L., Techkarnjanaruk S., Dohnalkova A., McCready D., Peyton B. M., and Geesey G. G. (2001) Iron sulfides and sulfur species produced at hematite surfaces in the presence of sulfate-reducing bacteria. *Geochim. Cosmochim. Acta* **65,** 223–235.

Nesbitt H. W. and Muir I. J. (1998) Oxidation states and speciation of secondary products on pyrite and arsenopyrite reacted with mine waste waters and air. *Mineral. Petrol.* **62,** 123–144.

Nesbitt H. W. and Banerjee D. (1998) Interpretation of XPS Mn(2p) spectra of Mn oxyhydroxides and constraints on the mechanism of MnO_2 precipitation. *Amer. Mineral.* **83,** 305–315.

Nesbitt H. W., Muir I. J., and Pratt A. R. (1995) Oxidation of arsenopyrite by air and air-saturated, distilled water, and implications for mechanism of oxidation. *Geochim. Cosmochim. Acta* **59,** 1773–1786.

Ngubane W. T. and Baecker A. A. W. (1990) Oxidation of gold-bearing pyrite and arsenopyrite by *Sulfolobus acidocaldarius* and *Sulfolobus* BC in airlift bioreactors. *Biorecovery* **1,** 255–269.

Nordstrom D. K. and Southam G. (1997) Geomicrobiology of sulfide oxidation. *Rev. Mineral.* **35,** 361–390.

Pratt A. R., Muir I. J., and Nesbitt H. W. (1994) X-ray photoelectron and Auger electron spectroscopic studies of pyrrhotite and mechanism of air oxidation. *Geochim. Cosmochim. Acta* **58,** 827–841.

Richardson S. and Vaughan D. J. (1989) Arsenopyrite: A spectroscopic investigation of altered surfaces. *Mineral. Mag.* **53,** 223–229.

Sampson M. I. and Blake R. C., II (1999) The cell attachment and oxygen consumption of two strains of *Thiobacillus ferrooxidans*. *Minerals Eng.* **12,** 671–686.

Sand W., Gerke T., Hallmann R., and Schippers A. (1995) Sulfur chemistry, biofilm, and the (in)direct attack mechanism—A critical evaluation of bacterial leaching. *Appl. Microbiol. Biotechnol.* **43,** 961–966.

Schaufuss A. G., Nesbitt H. W., Scaini M. J., Hoechst H., Bancroft M. G., and Szargan R. (2000) Reactivity of surface sites on fractured arsenopyrite (FeAsS) toward oxygen. *Am. Mineral.* **85,** 1754–1766.

Scofield J. H. (1976) Hartree-Slater subshell photoionization cross-sections at 1254 and 1487 eV. *J. Elec. Spec.* **8,** 129–137.

Seeger M. and Jerez C. A. (1992) Phosphate limitation affects global gene expression in *Thiobacillus ferrooxidans*. *Geomicrobiol. J.* **10,** 227–237.

Southam G. and Beveridge T. J. (1992) Enumeration of thiobacilli within pH-neutral and acidic mine tailings and their role in the development of secondary mineral soil. *Appl. Environ. Microbiol.* **58,** 1904–1912.

Stipp S. L. and Hochella M. F. Jr. (1991) Structure and bonding environments at the calcite surface as observed with X-ray photoelectron spectroscopy (XPS) and low energy electron diffraction (LEED). *Geochim. Cosmochim. Acta* **55,** 1723–1736.

Tsang T., Coyle G. J., Adler I., and Yin L. (1979) XPS studies of ion bombardment damage of iron-sulfur compounds. *J. Elec. Spec.* **16,** 389–396.

Tuovinen O. H. and Kelly D. P. (1972) Biology of *Thiobacillus ferrooxidans* in relation to the microbiological leaching of sulphide ores. *Z. Allg. Mikrobiol.* **12,** 311–346.

Tuovinen O. H., Bhatti T. M., Bigham J. M., Hallberg K. B., Garcia O. Jr., and Lindström E. B. (1994) Oxidative dissolution of arsenopyrite by mesophilic and moderately thermophilic acidophiles. *Appl. Environ. Microbiol.* **60,** 3268–3274.

Zachara J. M., Fredrickson J. K., Smith S. C., and Gassman P. L. (2001) Dissolution of Fe(III) oxide-bound trace metals by a dissimilatory Fe(III) reducing bacterium. *Geochim. Cosmochim. Acta* **65,** 75–93.